Asian Journal of Chemistry; Vol. 36, No. 1 (2024), 141-147

ASIAN JOURNAL OF CHEMISTRY

https://doi.org/10.14233/ajchem.2024.30708

A Comparative Study of Antioxidant and Antibacterial Activity of CuO, ZnO and Mixed (CuO/ZnO) Nanoparticles using *Cassia alata* Flower Extract

S. KARTHIKA[1,*], N. MANI[1], K. ANNAIDASAN[2], B. LATHA MAHESWARI[1], N. KAVIKALA[1] and V. RAJASUDHA[3]

[1]P.G. and Research Department of Chemistry, A.V.V.M. Sri Pushpam College (Affiliated to Bharathidasan University), Poondi, Thanjavur-613503, India
[2]Department of Geography, Central University of Tamilnadu, Thiruvarur-610005, India
[3]Department of Chemistry, Annai Vailankanni Arts and Science College (Affiliated to Bharathidasan University), Thanjavur-613007, India

*Corresponding author: E-mail: karchemistry28@gmail.com

Received: 14 October 2023; *Accepted*: 20 November 2023; *Published online*: 31 December 2023; AJC-21496

In the current scenario, environmental friendly methods of synthesizing nanoparticles and their composites have become a desirable trend. Phytochemicals derived from plant extracts are now being employed as a distinctive method for synthesizing nanoparticles due to their ability to serve as both reducing and capping agents. In present study, copper oxide nanoparticles (CuO NPs), zinc oxide nanoparticles (ZnO NPs) and their mixed composites (CuO/ZnO) were synthesized using the flower extract of plant *Cassia alata*. The synthesis of nanoparticles was confirmed by observing the colour change of the reaction mixture and was determined by detecting the surface plasmon resonance band at 280, 320 and 359 nm for CuO, ZnO and CuO/ZnO, respectively. The antioxidant activity of nanoparticles was characterized for DPPH, ABTS, NO and iron reducing power method. In addition, the antibacterial properties of these bioactive nanoparticles were also investigated. The CuO/ZnO nanocomposites showed superior antioxidant and antibacterial activity than CuO and ZnO nanoparticles.

Keywords: *Cassia alata*, Copper oxide nanoparticles, Zinc oxide nanoparticles, Nanocomposites, Biological activity.

INTRODUCTION

Nanoparticles because of their innate physical and chemical characteristics compared to its bulk form has created a fascination in their application in a variety of fields [1]. The nanomaterials with tuneable morphology and different composition display a variety of functions and novel properties. These nanomaterials exhibit prospective capabilities in drug delivery, sensing, imaging, separation, catalytic and as effective antioxidant and antibacterial agents [2-8]. Recently, a variety of nanoparticles including metal, metal oxides, metal chlorides and metal sulphides have been fabricated [9]. The process of synthesizing nanoparticles through the implementation of green chemistry principles involves the utilization of methodologies and procedures that strive to reduce or eradicate the use of harmful chemicals that may pose a risk to human well-beings and the ecosystem. Moreover, the green nanosynthesis methodology is straightforward and offers numerous benefits in contrast to physical and chemical approaches [1].

Copper oxide nanoparticles also exhibits high yields under moderate reaction conditions. They have short reaction time compared to conventional catalysts [10]. The synthesis of copper oxide nanoparticles using physical, chemical, thermal decomposition, electrochemical, photochemical, vacuum vapour deposition, sol-gel and irradiation methods has been reported [11,12]. The synthesis of copper oxide nanoparticles has been reported to involve a biological mode of nanosynthesis, which includes the participation of plants, bacteria and fungi [13]. Similarly, zinc oxide nanoparticles are highly effective as antibacterial and antimicrobials. Zinc oxide nanoparticles show excellent photocatalytic degradation and hence can be utilized as effective candidature in environmental remediation through photo catalysis [14,15]. The combination synthesis of metal oxide and metal nanoparticles gained considerable interest recently and made a major contribution to the advancement of nanomaterial chemistry [16]. A number of combinations of metallic elements and oxides, including zinc, titanium, graphene, magnesium oxides and ferrous sulphate have been found to serve as efficient supports [17-21].

The nanosynthesis approach with the use of biological entities involves the development and design of chemical materials and procedures that minimize the use of hazardous chemicals, which can potentially endanger the health of humans and the environment. The utilization of plant products is advantageous over other methods of nanosynthesis such as photochemical reduction [22], chemical reduction [23], thermal decomposition and thermochemical reduction [24]. The green route of nanosynthesis is cost effective, safe, simple and utilizes natural products for reduction [25-27]. The presence of alkaloids, phenolic compounds, polyphenols [28], carbohydrates [29], proteins [30,31], and terpenoids has been found to play a significant and effective role in reducing metal ions and stabilizing the resulting nanoparticles.

The plant *Cassia alata* (family: Fabaceae) is an important medicinal herb that is widely used by traditional medical practitioners in India and many parts of South-East Asia. Therapeutic properties such as anti-inflammatory, ability to eliminate water from bowels (hydragogue), induce sweating (sudorific), insecticidal and pesticidal activities have been reported [32]. Almost all parts of this plant, such as roots, leaves and flowers exhibit various biological activities. Fatmawati *et al*. [33] reviewed the antimicrobial, anticancer, expectorant and curing urinary tract infections functions of *C. alata*. Joshi [34] reported the plant to possess effective pharmacological properties in the treatment of asthma, constipation and bronchitis. Similarly, Varghese *et al.* [35] reported the use of *C. alata* leaves to treat malarial infection, yellow fever, *etc*. Further, the leaves are also used as antiasthmatic and in treating diabetes. The juice obtained from fresh leaves is effective in treating ringworm infections, snake and scorpion bites. The medicinal properties of *C. alata* was attributed to alkaloids, anthroquinones, flavonoids, tannins, terpenoids and sterols [36].

EXPERIMENTAL

Bright yellow coloured *C. alata* flowers were collected from Thanjavur, India and were taxonomically identified at Department of Botany, St. Joseph's College, Tiruchirappalli, India. The chemicals used in this study were of analytical grade chemicals procured from Sigma-Aldrich Pvt. Ltd.

Preparation of aqueous extract: To prepare the aqueous extract of *C. alata* flowers, a quantity of 5 g of dried flower powder was combined with 100 mL of deionized water in a 500 mL conical flask. The mixture was then heated to 60 ºC and boiled for 10 min. The solution underwent filtration utilizing Whatman filter paper No. 1 and was subsequently preserved at -4 ºC for further studies.

Synthesis of copper oxide nanoparticles: A 10 mL of 5% aqueous extract derived from *C. alata* flowers was introduced into a solution containing 40 mL of copper chloride (3 mM) with continuous stirring for a period of 24 h at 80 ºC, utilizing a magnetic stirrer. The formation o CuO NPs was established through the visual observation of a chromatic transition from a light to a dark brown hue. The centrifugation process lasted for a duration of 15 min at a speed of 10,000 revolutions per min. After decanting the supernatant, the solid was collected and dried at 80 ºC in oven [37].

Synthesis of zinc oxide nanoparticles: The protocol of Karimi *et al.* [38] was followed in the synthesis of ZnO NPs. In brief, 10 mL of 5% aqueous extract of *C. alata* flowers was added to 50 mL of 0.1 M zinc nitrate and heated the solution to 75 ºC for 2 h. Then the solution was allowed to cool to ambient temperature and centrifuged at a rate of 8000 rpm for 15 min. The collected solid residue was washed thoroughly using distilled water and again centrifuged for 10 min at a speed of 1000 rpm. The obtained white solid nanoparticles were oven-dried for 12 h at 70 ºC. The solid product was ground and calcined at 350 ºC for 10 min.

Synthesis of mixed CuO-ZnO nanoparticles: The mixed nanocomposite of copper oxide and zinc oxide was synthesized utilizing the modified protocol as described by Elemike *et al.* [39]. A solution of 400 mL of zinc acetate (10 mM) was added to 160 mL of 5% flower extract of *C. alata* followed by the addition of 10 mL of 1 N NaOH and then heated the solution to 80 ºC for 4 h, while being continuously agitated with a magnetic stirrer. The solution was allowed to equilibrate to ambient temperature, after which 400 mL of 2 mM solution of copper sulphate was added and then then heated the solution to 80 ºC for 4 h. After centrifugation, the solid product was separated, washed thoroughly with deionized water and then dried at 80 ºC in an oven for 48 h.

Characterization of nanoparticles

UV-Vis spectrophotometer analysis: Reduction of Cu, Zn and CuO-ZnO by *C. alata* flower extract and the resulting colour change indicated the formation of nanoparticles which were observed using UV-Vis spectroscopy. In order to assess the excitation of the reduced metal oxide, the specimen was diluted with distilled water and subjected to UV-visible spectrophotometry. The absorption maxima was then scanned within the 200-800 nm range, utilizing the Perkin-Elmer Lambda 2 UV 198 visible spectroscopy instrument.

Antioxidant activities: The DPPH radical scavenging and the total reducing power assay were evaluated following the protocol of Syed *et al.* [40]. Nitric oxide scavenging of synthesized nanoparticles and nanocomposites was evaluated by following the method of Hashemi & Ebrahimzadeh [41], whereas ABTS free radical inhibition was measured using Hajebi *et al.*'s method [42].

DPPH scavenging activity: The present study investigated the DPPH scavenging activity of *C. alata* flowers using CuO NPs, ZnO NPs and CuO/ZnO NPs. The experimental protocol employed was based on the methodology as described by Syed *et al.* [40] following with minor modifications. A 1 mL of 0.1 mM DPPH in ethanol was introduced into a test tube that contained varying concentrations (ranging from 10 to 50 µg/mL) of material. After agitation, the mixture was kept light-free for 30 min. The UV-visible spectrometry was utilized to read the optical density of the reacting mixture at 517 nm with respect to a blank (ethanol) and ascorbic acid was employed as standard. The following equation was used to deter-mine the percentage of inhibition of free radical:

$$\text{Inhibition (\%)} = \frac{\text{Control} - \text{Sample}}{\text{Control}} \times 100$$

ABTS assay: The ABTS radical scavenging assay of *C. alata* flowers mediated nanoparticles and nanocomposites were estimated in terms of the decolourization of the free radicals [42]. Briefly, equal volumes of the various concentrations (w/v) (10, 20, 30, 40 and 50 µg/mL) of nanoparticles/nanocomposites were combined with the freshly prepared ABTS solution (1 mL) vortexed for few seconds and incubated for 6 min. Absorbance of the sample at 734 nm was measured in triplicate. The scavenging activity was measured in terms of low absorbance.

Nitric oxide scavenging assay: In this study, 1 mL of nanoparticles/nanocomposites from *C. alata* flowers at various concentrations of 10, 20, 30, 40, and 50 µg/mL was added to 0.5 mL of sodium nitroprusside (5 mM) solution followed by phosphate buffered saline (PBS) solution (pH 7.4). The reaction mixture was incubated at 25 ºC for 150 min. The Griess reagent was utilized to measure the amount of nitrite produced from sodium nitroprusside and then the absorbance at 570 nm was measured quickly using a UV-visible spectrophotometer. The nitric oxide scavenging effect was quantified by comparing the absorbance values of the control and the positive standard (L-ascorbic acid) to determine the percentage using eqn. 2:

$$\text{Inhibition } (\%) = \frac{\text{Control} - \text{Sample}}{\text{Control}} \times 100 \qquad (2)$$

Reducing power assay: In this assay, different concentrations of nanoparticles and nanocomposites in the range between 10 to 50 µg/mL were used. To 1 mL of sample, 2.5 mL of 1% potassium ferricyanide (2.5 mL) and 0.2 M phosphate buffer (pH = 6.6) were added and incubated at 50 ºC for 20 min. A 2.5 mL of 10% TCA was added to stop the reaction and then centrifuged the mxiture for 10 min. Following centrifugation, a volume of 2.5 mL of the resulting supernatant was combined with equal amounts of distilled water and ferric chloride (0.1 mL). L-Ascorbic acid was used as standard and the absorbance was determined at a wavelength of 700 nm [40].

Antibacterial activity: The susceptibility of both Gram-negative bacteria, namely *Escherichia coli* and *Klebsiella pneumoniae*, as well as Gram-positive bacteria, specifically *Staphylococcus aureus* and *Streptococcus pneumoniae,* were assessed using *C. alata* flower extract-mediated CuO NPs, ZnO NPs and mixed CuO/ZnO NPs. The nutrient agar medium was utilized to conduct the Agar well diffusion assay. The bacterial strains were standardized to a 0.5 McFarland standard, which corresponds to a concentration of 1×10^8 CFU mL^{-1}. The standardized bacterial strains were then evenly distributed on the sterile nutrient agar plates. The plates were dried for 15 min before the susceptibility tests were performed. Wells with a diameter of 6 mm were created on nutrient agar and subsequently filled with CuO NPs, ZnO NPs, CuO/ZnO NPs and 20 L of crude extract. The antibiotic amoxicillin was utilized as a positive control in the experiment. Following a 24 h incubation period at 37 ºC, the measurement of the zone of inhibition was conducted.

RESULTS AND DISCUSSION

The copper oxide nanoparticles were synthesized with aqueous flower extract of *C. alata* by addition of 5% aqueous flower extract to copper chloride solution. The reacting solution turned to a dark brown colour with the addition of flower extract. The aqueous leaf extract of *S. auriculata* showed the formation of a dark brown colour, indicating the formation of copper oxide nanoparticles was in agreement with the present observation. In present study, the aqueous flower extract of *C. alata* mediated CuO NPs exhibited a SPR absorbance peak measured at a wavelength A λ_{max} = 280 nm (Fig. 1), which is in agreement with the previous reports [43-45].

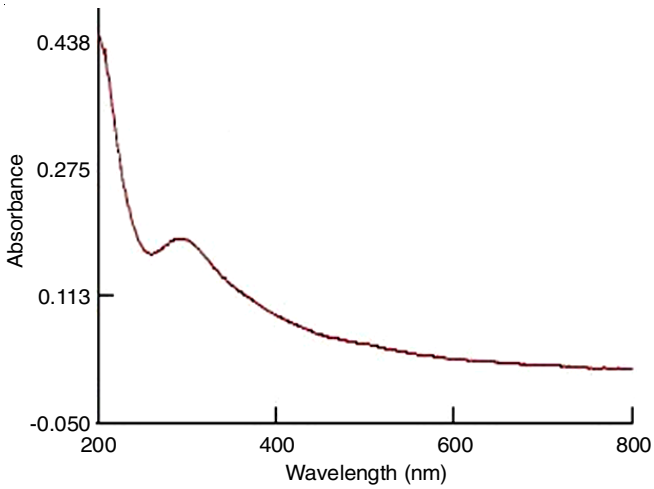

Fig. 1. UV-visible absorption spectrum of CuO nanoparticles mediated through *C. alata* flowers

The confirmation of the formation of zinc oxide nanoparticles was established through direct visual inspection, as indicated by the significant alteration in the color of the solution from brown to a light white colour. A change in colour to light white during the formation of ZnO NPs using a aqueous extract of *C. alata* flower was accompanied by a strong absorption peak at 320 nm (Fig. 2). The reduction of zinc ions into zinc oxide nanoparticles is attributed to the presence of phytochemicals such as flavonoids, tannins, terpenoids, cardiac glycosides and steroids in *C. alata* [46].

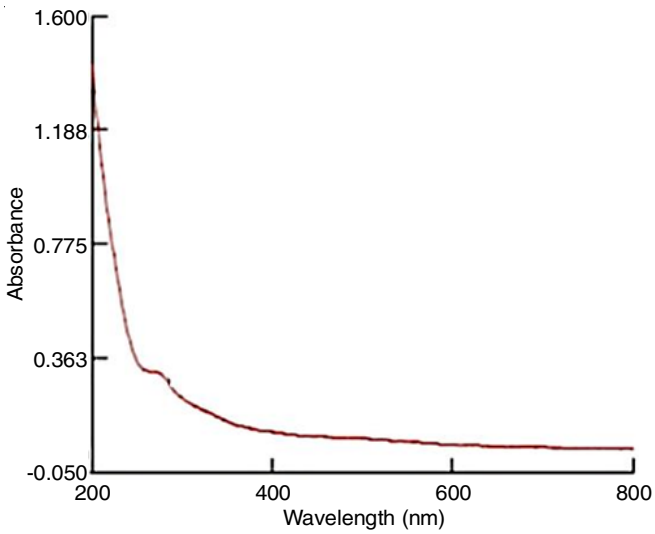

Fig. 2. UV-visible absorption spectrum of ZnO nanoparticles mediated through *C. alata* flowers

The reduction of copper and zinc ions to copper oxide and zinc oxide nanoparticles, respectively was monitored using UV-visible spectroscopy in wavelength ranging between 200-800 nm. The reaction mixture underwent a change in colour transitioning from a pale brown colour to a deep brown colour, which is attributed to the vibration of surface plasmon resonance. The *C. alata* aqueous flower extract mediated nanocomposite exhibited a SPR peak at wavelength of 359 nm (Fig. 3). The absorption peak for CuO/ZnO nanocomposite was lower in the ultraviolet region and shifted and broaden in the visible region compared to pure ZnO nanoparticles. The interfacial coupling between the CuO and ZnO nanoparticles might have caused this shift in plasmon absorption.

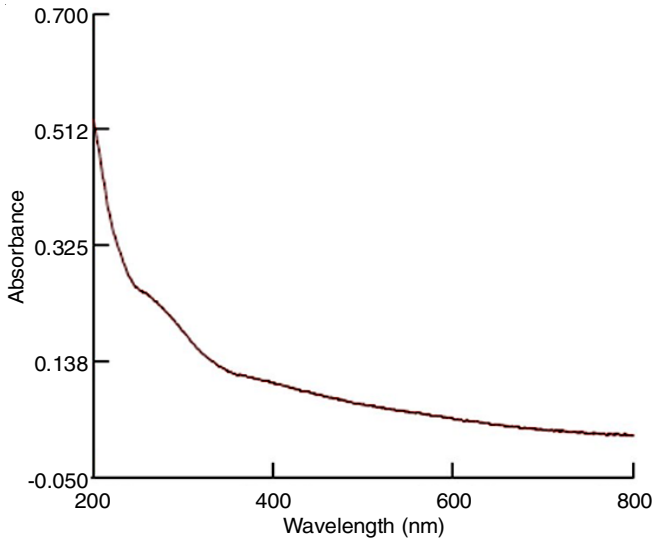

Fig. 3. UV-visible absorption spectrum of CuO/ZnO nanocomposite mediated through *C. alata* flowers

Antioxidant activities: Table-1 represents the DPPH scavenging activity of CuO NPs mediated through the aqueous flower extract of *C. alata*. A colour change from purple to yellow with the addition of CuO NPs indicated the completion of DPPH free radical quenching by CuO NPs, which was measured spectrophotometrically at 517 nm. The DPPH free radical scavenging activity of CuO NPs ranged between 29.21 to 50.94% with increasing concentration of CuO NPs. Maximum DPPH scavenging activity of 50.94% was observed with 50 µg/mL concentration. The IC_{50} value of CuO NPs against DPPH was 54.696 µg/mL and 24.90% of ABTS free radicals were scavenged with 10 µg/mL concentration of CuO NPs. A gradual increase in ABTS scavenging activity by CuO NPs was evident and at 50 µg/mL concentration of CuO NPs, ABTS scavenging activity was found to be 46.85%. The IC_{50} value of CuO NPs against ABTS free radicals was found to be 54.696 µg/mL. The scavenging activity of CuO NPs was found to be low compared to the standard, ascorbic acid. The *C. alata* mediated CuO NPs showed 30.98% of NO free radical scavenging activity at 10 µg/mL concentration. A gradual increase in NO radical scavenging activity by CuO NPs was evident and at 50 µg/mL concentration of biogenic copper oxide nanoparticles, NO scavenging activity was found to be 49.83%. The IC_{50} value of CuO NPs against NO free radicals was found to be 66.04 µg/mL. The reduction of Fe^{3+} was found to be dose dependent. The CuO NPs at 10 µg/mL exhibited 27.17% of reduction potential. At 50 µg/mL concentration, CuO NPs had a maximum reduction potential of 42.92%. The IC_{50} value of reduction potential was reported to be 47.807 µg/mL with CuO NPs.

The reductive effect of *C. alata* mediated CuO NPs increased with increasing concentration of dosage. The reducing power of CuO NPs was observed to be close to the control (Fig. 4) indicating the possible role of hydrophilic polyphenolic compounds present in *C. alata* that surrounded the synthesized CuO NPs which exerted high reducing power [47]. The present study observed that ascorbic acid is effective in quenching the free radicals compared to the *C. alata* mediated CuO NPs. This low antioxidant activity of CuO NPs compared to ascorbic acid may be attributed to the difference in the concentration of phytochemicals present in the flowers of *C. alata*.

The enhanced antioxidant activity exhibited by ZnO NPs in comparison to its bulk counterparts can be attributed to the increased surface area to volume ratio. The current study investigated the antioxidant properties of ZnO NPs synthesized using *C. alata* flower extract, which demonstrated significant efficacy in scavenging free radicals. The DPPH reduction process causes a substantial change in the colour of the reaction mixture, shifting from purple to yellow. This shift can be precisely quantified and evaluated using UV-visible spectroscopy, specifically by determining the wavelength at which maximum absorption (λ_{max}) occurs at 517 nm [48]. The IC_{50} value of DPPH was determined to be 33.570 µg/mL, in the same way, the ABTS assay yielded a value of 41.125 µg/mL, while the NO assay resulted in a value of 71.554 µg/mL. The ferrous reducing power was determined to be 42.383 µg/mL. The observed quenching of DPPH radicals may be attributed to the electron transfer process from oxygen to the unpaired electron in the nitrogen atom of DPPH. This electron transfer leads to a decrease in the transition intensity at 517 nm, following the $n \rightarrow \pi$ transition [49]. Therefore, the antioxidant activity is contingent upon the capacity to donate hydrogen. The reducing power assay is utilized to determine the transfer of an electron and the subsequent reduction of oxidized intermediates of lipid peroxidase.

TABLE-1
ANTIOXIDANT ACTIVITY OF *C. alata* FLOWER EXTRACT MEDIATED CuO NPs

Antioxidant assay	Inhibition of free radicals (%)					IC_{50} value
	10 µg/mL	20 µg/mL	30 µg/mL	40 µg/mL	50 µg/mL	
DPPH	29.21 ± 1.23	33.22 ± 1.31	39.20 ± 1.35	44.07 ± 0.65	50.94 ± 1.66	54.696
ABTS	24.90 ± 1.26	29.08 ± 1.24	34.96 ± 1.29	41.73 ± 1.80	46.85 ± 1.81	54.696
NO	30.98 ± 1.24	36.12 ± 0.56	43.38 ± 1.04	46.47 ± 1.27	49.83 ± 0.07	66.040
Red.Power	27.17 ± 0.65	30.94 ± 1.26	35.25 ± 1.20	39.02 ± 1.67	42.92 ± 1.51	47.807

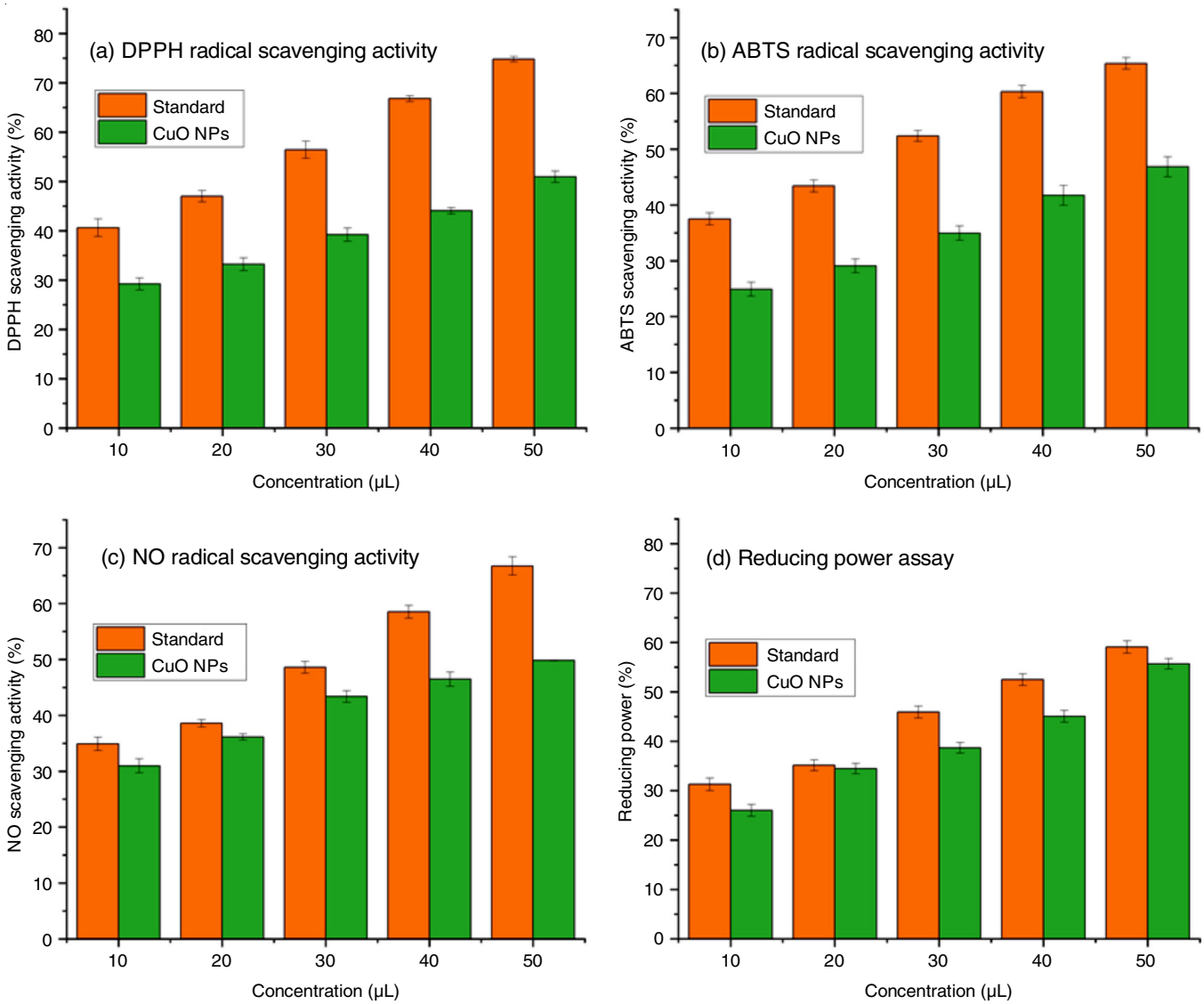

Fig. 4. Antioxidant potential of CuO NPs mediated through aqueous flower extract of *C. alata*

In current study, the test solution underwent a colour change from yellow to green and blue at a wavelength of 700 nm. This transformation was attributed to the conversion of ferrous ions by the reducers, which were present in different concentrations of ZnO NPs. The observed trend of increasing reducing power as the concentration of ZnO NPs increases suggests the existence of electron-donating compounds within ZnO NPs that can effectively interact with free radicals, thereby terminating the chain reactions initiated by these radicals [50]. The IC_{50} value for the reducing power of ZnO NPs was determined to be 42.383 µg/mL. The observed phenomenon of ZnO NPs exhibiting a capacity to absorb NO was determined to be contingent upon the dosage administered. No scavenging activity was detected at a concentration of 50 µg/mL as indicated in Table-2.

The *C. alata* mediated mixed nanocomposites (CuO/ZnO NPs) antioxidant activity is presented in Table-3. The percentage of DPPH radical scavenging activity of CuO/ZnO nanocomposite was observed to be 64.3% at maximum concentration evaluated in the present study, which concluded that CuO/ZnO NPs exhibited 14% more than ZnO NPs. The nanocomposite showed better scavenging activity with IC_{50} value of 27.708 (DPPH), 29.620 (ABTS) 44.246 (NO) and 36.883

TABLE-2
ANTIOXIDANT ACTIVITY OF *C. alata* FLOWER EXTRACT MEDIATED ZnO NPs

Antioxidant assay	Inhibition of free radicals (%)					IC_{50} value
	10 µg/mL	20 µg/mL	30 µg/mL	40 µg/mL	50 µg/mL	
DPPH	33.37 ± 1.09	40.37 ± 1.21	47.19 ± 1.45	55.06 ± 0.61	61.51 ± 1.16	33.570
ABTS	30.34 ± 1.53	37.03 ± 0.44	43.10 ± 1.07	48.62 ± 1.09	55.96 ± 1.06	41.125
NO	27.28 ± 1.85	32.48 ± 1.09	37.36 ± 1.10	44.17 ± 0.52	51.29 ± 1.45	71.554
Red.Power	24.93 ± 1.20	32.92 ± 1.29	32.94 ± 1.27	38.53 ± 1.14	39.65 ± 1.07	42.283

TABLE-3
ANTIOXIDANT ACTIVITY OF *C. alata* FLOWER EXTRACT MEDIATED CuO/ZnO NPs

Antioxidant assay	Inhibition of free radicals (%)					IC_{50} value
	10 µg/mL	20 µg/mL	30 µg/mL	40 µg/mL	50 µg/mL	
DPPH	37.12 ± 1.14	44.37 ± 1.75	52.17 ± 1.75	59.39 ± 1.09	64.30 ± 1.96	27.708
ABTS	34.180 ± 1.70	43.82 ± 1.74	50.94 ± 1.22	58.50 ± 1.25	64.05 ± 0.48	29.620
NO	24.27 ± 1.11	35.40 ± 1.08	44.49 ± 1.26	52.27 ± 1.81	62.19 ± 1.03	44.246
Red.Power	26.00 ± 1.26	34.47 ± 1.05	38.66 ± 1.06	45.05 ± 1.19	55.64 ± 1.05	36.883

TABLE-4
ANTIBACTERIAL ACTIVITY OF *C. alata* FLOWER EXTRACT AND NANOPARTICLES

Bacteria	Antibiotic	Zone of inhibition (mm)			
		Extract	CuO NPs	ZnO NPs	CuO/ZnO NPs
S. aureus	14.0	14.5	14.9	12.5	15.0
E. coli	14.5	14.2	17.5	16.5	18.0
K. pneumoniae	15.0	14.4	15.0	14.0	14.0
S. pneumoniae	14.5	14.6	15.0	14.8	16.5

µg/mL (reducing power), which was much lower compared to the IC_{50} values recorded by CuO NPs and ZnO NPs in the present study. However, the present study observed a comparatively low activity than the standard ascorbic acid.

Antibacterial activity: The antibacterial activity data of *C. alata* flower extract mediated CuO NPs, ZnO NPs and CuO/ZnO NPs is presented in Table-4. A high antibacterial activity was observed with nanocomposite, followed by CuO NPs and ZnO NPs. The nanoparticles were highly effective against *E. coli* and the bacteriostatic zone formed by CuO NPs was 17.5 mm, ZnO NPs (16.5 mm) and CuO/ZnO NPs (18.0 mm). It was found that *Streptococcus pneumoniae* exhibited susceptibility to synthesize nanoparticles in order of ZnO NPs, CuO NPs and CuO/ZnO with the zone of inhibition measuring 14.8, 15.0 and 16.5 mm, respectively. Multi-drug resistant *Staphylococcus aureus* was least susceptible to nanoparticles with the zone of inhibition measuring 14.9 mm (CuO NPs), 12.5 mm (ZnO NPs) and 15.0 mm (CuO/ZnO).

Conclusion

The present study signifies that *C. alata* flowers have a vast variety of secondary metabolites that can be exploited for the synthesis of environmentally benign nanoparticles and nanocomposites. The CuO NPs, ZnO NPs and their mixed nanocomposite (CuO/ZnO NPs) exhibited effective antioxidant and antimicrobial activities. Hence, these nanoparticles can be utilized as an alternative to synthetic/commercial antioxidants as well as antimicrobials.

CONFLICT OF INTEREST

The authors declare that there is no conflict of interests regarding the publication of this article.

REFERENCES

1. S. Gul, M. Ismail, M.I. Khan, S.B. Khan, A.M. Asiri, I.U. Rahman, M.A. Khan and M.A. Kamboh, *Asian Pac. J. Trop. Dis.*, **6**, 311 (2016); https://doi.org/10.1016/S2222-1808(15)61036-2
2. N. Chen, Y. Huang and Y. Wang, *Biomaterials*, **35**, 9709 (2014); https://doi.org/10.1016/j.biomaterials.2014.08.017
3. R. Sankar, R. Maheswari, S. Karthik, K.S. Shivashangari and V. Ravikumar, *Mater. Sci. Eng. C*, **44**, 234 (2014); https://doi.org/10.1016/j.msec.2014.08.030
4. Z. Ji, X. Shen, G. Zhu, H. Zhou and A. Yuan, *J. Mater. Chem.*, **22**, 3471 (2012); https://doi.org/10.1039/c2jm14680k
5. M. De, P.S. Ghosh and V.M. Rotello, *Adv. Mater.*, **20**, 4225 (2008); https://doi.org/10.1002/adma.200703183
6. R. Costi, A.E. Saunders and U. Banin, *Angew. Chem. Int. Ed.*, **49**, 4878 (2010); https://doi.org/10.1002/anie.200906010
7. X. Wang, H. Zhu, Y. Bao, F. Yang and X. Yang, *ACS Nano*, **5**, 3250 (2011); https://doi.org/10.1021/nn2003794
8. D. Wang and Y. Li, *Adv. Mater.*, **23**, 1044 (2011); https://doi.org/10.1002/adma.201003695
9. V. Gopinath, S. Priyadarshini, N. Meera Priyadharsshini, K. Pandian and P. Velusamy, *Mater. Lett.*, **91**, 224 (2013); https://doi.org/10.1016/j.matlet.2012.09.102
10. M. Salavati-Niasari, F. Davar and N. Mir, *Polyhedron*, **27**, 3514 (2008); https://doi.org/10.1016/j.poly.2008.08.020
11. Y. Zhao, J.-J. Zhu, J.-M. Hong, N. Bian and H.-Y. Chen, *Eur. J. Inorg. Chem.*, **2004**, 4072 (2004); https://doi.org/10.1002/ejic.200400258
12. M.-S. Yeh, Y.-S. Yang, Y.-P. Lee, H.-F. Lee, Y.-H. Yeh and C.-S. Yeh, *J. Phys. Chem. B*, **103**, 6851 (1999); https://doi.org/10.1021/jp984163+
13. K.M. Rajesh, B. Ajitha, Y.A.K. Reddy, Y. Suneetha and P.S. Reddy, *Optik*, **154**, 593 (2018); https://doi.org/10.1016/j.ijleo.2017.10.074
14. J. Singh, T. Dutta, K.-H. Kim, M. Rawat, P. Samddar and P. Kumar, *J. Nanobiotechnology*, **16**, 84 (2018); https://doi.org/10.1186/s12951-018-0408-4
15. J. Singh, S. Kumar, A. Alok, S.K. Upadhyay, M. Rawat, D.C.W. Tsang, N. Bolan and K.-H. Kim, *J. Clean. Prod.*, **214**, 1061 (2019); https://doi.org/10.1016/j.jclepro.2019.01.018
16. A. Goswami, A.K. Rathi, C. Aparicio, O. Tomanec, R. Pocklanova, M. Petr, M.B. Gawande, R.S. Varma and R. Zboril, *ACS Appl. Mater. Interfaces*, **9**, 2815 (2017); https://doi.org/10.1021/acsami.6b13138
17. I. Udom, Y. Zhang, M.K. Ram, E.K. Stefanakos, A.F. Hepp, R. Elzein, R. Schlaf and D.Y. Goswami, *Thin Solid Films*, **564**, 258 (2014); https://doi.org/10.1016/j.tsf.2014.05.057
18. K. Mori, K. Miyawaki and H. Yamashita, *ACS Catal.*, **6**, 3128 (2016); https://doi.org/10.1021/acscatal.6b00715
19. M. Nasrollahzadeh, S. Mohammad Sajadi, A. Rostami-Vartooni, M. Alizadeh and M. Bagherzadeh, *J. Colloid Interface Sci.*, **466**, 360 (2016); https://doi.org/10.1016/j.jcis.2015.12.036

20. M. Nasrollahzadeh and S.M. Sajadi, *J. Colloid Interface Sci.*, **464**, 147 (2016); https://doi.org/10.1016/j.jcis.2015.11.020
21. M. Pudukudy, Z. Yaakob, M.Z. Mazuki, M.S. Takriff and S.S. Jahaya, *Appl. Catal. B*, **218**, 298 (2017); https://doi.org/10.1016/j.apcatb.2017.04.070
22. X. Zhu, B. Wang, F. Shi and J. Nie, *Langmuir*, **28**, 14461 (2012); https://doi.org/10.1021/la303244p
23. Q. Zhang, Z.-M. Yang, B. Ding, X. Lan and Y. Guo, *Trans. Nonferrous Met. Soc. China*, **20**, s240 (2010); https://doi.org/10.1016/S1003-6326(10)60047-7
24. R. Betancourt-Galindo, P.Y. Reyes-Rodriguez, B.A. Puente-Urbina, C.A. Avila-Orta, O.S. Rodriguez-Fernandez, G. Cadenas-Pliego, R.H. Lira-Saldivar and L.A. Garcia-Cerda, *J. Nanomater.*, **2014**, 980545 (2014); https://doi.org/10.1155/2014/980545
25. B. Delma, B. Vijila and M. Jaya, *Int. J. Scientific Res. Publ.*, **6**, 134 (2016).
26. J.I. Abd-Elkareem, H.M. Bassuony, S.M. Mohammed, H.M. Fahmy and N.R. Abd-Elkader, *J. Bionanosci.*, **10**, 15 (2016); https://doi.org/10.1166/jbns.2016.1350
27. A.A. El-Refai, G.A. Ghoniem, A.Y. El-Khateeb and M.M. Hassaan, *J. Nanostruct. Chem.*, **8**, 71 (2018); https://doi.org/10.1007/s40097-018-0255-8
28. N. Ahmad, S. Sharma, M.K. Alam, V.N. Singh, S.F. Shamsi, B.R. Mehta and A. Fatma, *Colloids Surf. B Biointerfaces*, **81**, 81 (2010); https://doi.org/10.1016/j.colsurfb.2010.06.029
29. J. Kasthuri, S. Veerapandian and N. Rajendiran, *Colloids Surf. B Biointerfaces*, **68**, 55 (2009); https://doi.org/10.1016/j.colsurfb.2008.09.021
30. V. Kumar and S.K. Yadav, *Int. J. Green Nanotechnol.*, **3**, 281 (2011); https://doi.org/10.1080/19430892.2011.633474
31. S. Si and T.K. Mandal, *Chem. Eur. J.*, **13**, 3160 (2007); https://doi.org/10.1002/chem.200601492
32. C.A. Alalor, C.I. Igwilo and E. Jeroh, *J. Pharm. Allied Health Sci.*, **2**, 40 (2012).
33. S. Fatmawati, Yuliana, A.S. Purnomo and M.F. Abu Bakar, *Heliyon*, **6**, e04396 (2020); https://doi.org/10.1016/j.heliyon.2020.e04396
34. S.G. Joshi, Medicinal Plants, Oxford and IBH Publishing (2000).
35. G.K. Varghese, L.V. Bose and S. Habtemariam, *Pharm. Biol.*, **51**, 345 (2013); https://doi.org/10.3109/13880209.2012.729066
36. V.S. Neharkar and K.G. Gaikwad, *Res. J. Pharm. Biol. Chem. Sci.*, **2**, 783 (2011).
37. M.K. Ghosh, S. Sahu, I. Gupta and T.K. Ghorai, *RSC Adv.*, **10**, 22027 (2020); https://doi.org/10.1039/D0RA03186K
38. N. Karimi, M. Behbahani, G. Dini and A. Razmjou, *Adv. Nat. Sci.: Nanosci. Nanotechnol.*, **9**, 045009 (2018); https://doi.org/10.1088/2043-6254/aaf1af
39. E.E. Elemike, D.C. Onwudiwe and M. Singh, *J. Inorg. Organomet. Polym. Mater.*, **30**, 400 (2020); https://doi.org/10.1007/s10904-019-01198-w
40. A. Syed, N. Benit, A.A. Alyousef, A. Alqasim and M. Arshad, *Saudi J. Biol. Sci.*, **27**, 757 (2020); https://doi.org/10.1016/j.sjbs.2019.12.031
41. Z. Hashemi and M.A. Ebrahimzadeh, *Lat. Am. Appl. Res.*, **44**, 203 (2014); https://doi.org/10.52292/j.laar.2014.442
42. S. Hajebi, M.H. Tabrizi, M.N. Moghaddam, F. Shahraki and S. Yadamani, *J. Biol. Inorg. Chem.*, **24**, 395 (2019); https://doi.org/10.1007/s00775-019-01655-4
43. L.-B. Shi, P.-F. Tang, W. Zhang, Y.-P. Zhao, L.-C. Zhang and H. Zhang, *Trop. J. Pharm. Res.*, **16**, 185 (2017); https://doi.org/10.4314/tjpr.v16i1.25
44. H. Ahmad, K. Venugopal, A.H. Bhat, K. Kavitha, A. Ramanan, K. Rajagopal, R. Srinivasan and E. Manikandan, *Pharm. Res.*, **37**, 246 (2020); https://doi.org/10.1007/s11095-020-02966-x
45. S. Nazima Banu, *Int. J. Eng. Appl. Sci. Technol.*, **4**, 365 (2019).
46. H. Hazni, N. Ahmad, Y. Hitotsuyanagi, K. Takeya and C.-Y. Choo, *Planta Med.*, **74**, 1802 (2008); https://doi.org/10.1055/s-0028-1088340
47. D. Das, B.C. Nath, P. Phukon and S.K. Dolui, *Colloids Surf. B Biointerfaces*, **101**, 430 (2013); https://doi.org/10.1016/j.colsurfb.2012.07.002
48. R. Amarowicz, R.B. Pegg, P. Rahimi-Moghaddam, B. Barl and J.A. Weil, *Food Chem.*, **84**, 551 (2004); https://doi.org/10.1016/S0308-8146(03)00278-4
49. H.R. Madan, S.C. Sharma, Udayabhanu, D. Suresh, Y.S. Vidya, H. Nagabhushana, H. Rajanaik, K.S. Anantharaju, S.C. Prashantha and P. Sadananda Maiya, *Spectrochim. Acta A Mol. Biomol. Spectrosc.*, **152**, 404 (2016); https://doi.org/10.1016/j.saa.2015.07.067
50. B.N. Singh, A.K.S. Rawat, W. Khan, A.H. Naqvi and B.R. Singh, *PLoS One*, **9**, e106937 (2014); https://doi.org/10.1371/journal.pone.0106937